

Article

Sustainable Steel Carburization by Using Snack Packaging Plastic Waste as Carbon Resources

Songyan Yin *, Ravindra Rajarao, Farshid Pahlevani  and Veena Sahajwalla

Centre for Sustainable Materials Research and Technology (SMaRT), School of Materials Science and Engineering, UNSW Australia, Sydney NSW 2052, Australia; r.rajarao@unsw.edu.au (R.R.); f.pahlevani@unsw.edu.au (F.P.); veena@unsw.edu.au (V.S.)

* Correspondence: songyan.yin@student.unsw.edu.au; Tel.: +61-434-202-876

Received: 13 December 2017; Accepted: 17 January 2018; Published: 22 January 2018

Abstract: In recent years, the research regarding waste conversion to resources technology has attracted growing attention with the continued increase of waste accumulation issues and rapid depletion of natural resources. However, the study, with respect to utilizing plastics waste as carbon resources in the metals industry, is still limited. In this work, an environmentally friendly approach to utilize snack packaging plastic waste as a valuable carbon resources for steel carburization is investigated. At high temperature, plastic waste could be subject to pyrolytic gasification and decompose into small molecular hydrocarbon gaseous products which have the potential to be used as carburization agents for steel. When heating some snack packaging plastic waste and a steel sample together at the carburization temperature, a considerable amount of carbon-rich reducing gases, like methane, could be liberated from the plastic waste and absorbed by the steel sample as a carbon precursor for carburization. The resulting carburization effect on steel was investigated by optical microscopy, scanning electron microscopy, electron probe microanalyzer, and X-ray photoelectron spectrometer techniques. These investigation results all showed that snack packaging plastic waste could work effectively as a valuable carbon resource for steel carburization leading to a significant increase of surface carbon content and the corresponding microstructure evolution in steel.

Keywords: sustainable steel carburization; packaging plastic waste; carbon resources; methane

1. Introduction

Steel carburization is a widely-used case hardening method to enhance steel wear, corrosion, and fatigue resistance without sacrificing its toughness and machinability [1]. It is a process in which low carbon steel is immersed in a carbon-rich atmosphere to make activated free carbon deposit on the steel surface and be absorbed under the condition of high temperature [2]. Modern carburizing processes are dominated by high-temperature gas carburization, which uses natural gas consisting primarily of methane to serve as the carbon resource for steel carburization [3]. However, taking account of the ever-increasing world energy demand, but the dramatic decline of natural gas reserves, it is of vital importance to explore alternative carbon resources for steel carburization [4]. Plastics waste, a carbon-based material derived from petrochemicals, has a significant potential to be used as a carburizing agent for steel carburization.

Plastics are a group of synthetic materials consisting of carbon as a sole or major element [5]. Their rapidly-growing consumption in modern society has inevitably given rise to a large quantity of corresponding waste accumulation [6]. Over the past few decades, the urgency to recover resources from waste plastics has gained unprecedented attention around the world [7–9]. However, the technique concerning the reuse of complex snack packaging plastic waste is still not feasible due to its heterogeneous composite constitution and unavoidable external contamination [10–12]. Heating plastic

waste together with a steel sample at elevated carburization temperatures under an oxygen-free environment could subject plastic waste to pyrolytic gasification and decompose into small molecular hydrocarbon gases [13]. The small molecular hydrocarbon gases, like methane, could, in turn, work as valuable carbon resources for steel carburization. This sustainable carburization practice would not only alleviate the consumption of natural gas used in the conventional gas carburization of steel, but can also reduce the accumulation of plastics waste.

In this work, an environmentally friendly approach to carburize steel samples by using snack packaging plastic waste as a carbon resources is reported. When treating a steel sample together with the post-consumer snack packaging plastic in a horizontal tube furnace, the plastic waste was subjected to high-temperature pyrolytic gasification and generated carbon-rich reducing gases, such as CH₄ and CO, which can be absorbed by the steel sample as a carbon precursor for carburization. The carburization mechanism of this approach was studied via continuous monitoring of the primary reaction gases, like CH₄, CO, and CO₂, liberated from the plastic waste by an infrared gas analyzer. The carburization effect of plastic waste on the steel sample was investigated via microstructure evolution by optical microscopy (OM) and scanning electron microscopy (SEM), quantitative carbon content against depth profile determination by an electron probe microanalyzer (EPMA), and X-ray photoelectron spectrometry (XPS). These investigation results all showed that snack packaging plastic waste could work effectively as a valuable carbon resource for steel carburization and lead to a significant increase of surface carbon content, as well as the corresponding microstructure evolution in steel.

2. Materials and Methods

2.1. Materials

A reference steel sample with a carbon content of 0.39%, diameter of 4 mm, length of 10 mm, and a weight of 1g was used as a carburizing object in this study. Its detailed chemical composition was identified by a carbon sulfur analyzer (CS-230, LECO, Saint Joseph, MI, USA), inductively-coupled plasma optical emission spectroscopy (ICP-OES, 7300, PerkinElmer, Waltham, MA, USA) and inductively-coupled plasma mass spectrometry (ICP-MS, NexION, PerkinElmer, Waltham, MA, USA). The elemental composition result of the steel sample is listed in Table 1.

Table 1. Elemental composition of the reference steel sample used in this study.

Element	wt. %
C	0.39
Fe	98.95
Mn	0.564
Cu	0.108
Cr	0.085
Ni	0.06
Mo	0.019
Ca	0.015
Zn	0.005
Al	0.004
Ba	0.004
Co	0.004
As	0.003

One of the most popular snack packaging plastic waste, a post-consumer chips bag as shown in Figure 1a, was collected and manually shredded into small pieces typically of the size <1 cm² to utilize as a carbon precursor for steel carburization. Its chemical composition was determined by a LECO analyzer and ICP-OES; crystallographic constitution was characterized by the X-ray diffraction technique (XRD, MPD, PANalytical, Almelo, Netherlands); the polymer type of the plastic

contained was identified by Fourier transform infrared spectrometer (FTIR, Spectrum 100, PerkinElmer, Waltham, MA, USA). The thermal degradation behavior of the plastic waste was characterized by a thermogravimetric analyzer (TGA, STA 8000, PerkinElmer, Waltham, MA, USA) under an inert atmosphere in a temperature range of 30–1200 °C at a heating rate of 10 °C/min.

2.2. Experimental Methods

The schematic diagram of carburization experimental setup is shown in Figure 1. A reference steel sample (Figure 1b) and 0.8 g shredded packaging plastics waste (Figure 1a) was placed together into a covered alumina crucible as a carburization assembly. A horizontal tube furnace (Ceramic Engineering, Sydney, Australia) was adapted in this study for high temperature sustainable carburization process. High-purity (99.9%) argon gas was introduced at a flow rate of 1 L/min into the furnace to employ as a carrier gas. Firstly, the carburization assembly was placed into the cold zone (~300 °C) of the furnace for 5 min to avoid thermal shock. After that, the samples were pushed into the hot zone with a preset temperature of 1200 °C of the surface over 10 min of reaction. Finally, the samples were removed from the hot zone and backed to the cold zone for another 5 min to allow the steel sample to cool down in an inert atmosphere. The gaseous products, methane, carbon monoxide, and carbon dioxide, generated during this process, were monitored by an infrared gas analyzer (IR, AO2020, ABB, Zurich, Switzerland).

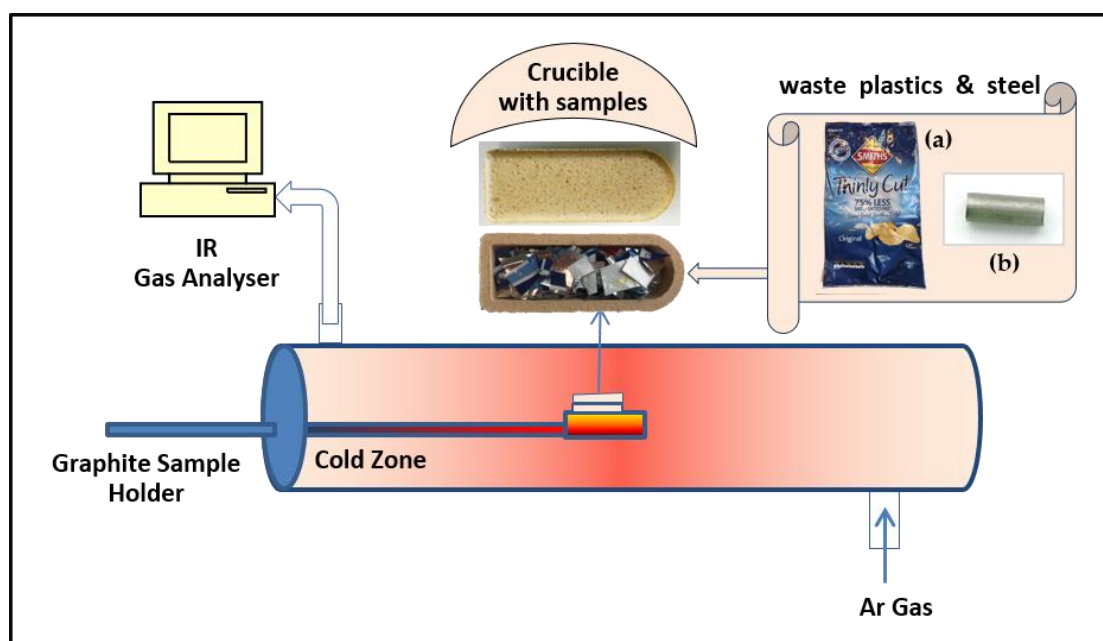


Figure 1. Schematic representation of carburization experiment.

2.3. Characterization of Carburization Effect of Plastic Waste on Steel

The microstructure evolution of steel was investigated by OM (EM600L, Nikon, Tokyo, Japan) and SEM (3400, Hitachi, Tokyo, Japan). The chemical state of carbon as well as its content against depth profile was studied using XPS (ESCALAB250Xi, Thermo Fisher Scientific, Waltham, MA, USA). The quantitative carbon distribution in steel was measured by EPMA (JXA-8500F, JEOL, Peabody, MA, USA) fitted with four wavelength-dispersive spectrometers and a silicon drift detector energy-dispersive spectrometer (SDD-EDS, JEOL, Peabody, MA, USA).

3. Results and Discussion

3.1. Characterisation of Snack Packaging Plastic Waste

The crystallographic characterization of post-consumer chips packaging plastic bag determined by XRD is given in Figure 2a. It revealed the plastic waste was mainly composed of polymer, aluminum and a trace amount of titanium dioxide. The polymer is of semi-crystalline characterized by a series of peaks in the range of 10° to 25° . The peaks positioned at 38.5° , 44.7° , 65.1° , and 78.2° unveil the aluminum foil contained in this snack packaging plastic is in a metal state. A trace amount of rutile titanium dioxide, which is widely used in the plastic products as a pigment [14], was found by the presence of weak peaks located at 27.4° , 36.1° , 41.2° , 54.3° , and 56.6° . The specific type of the polymer contained in this plastic waste was further identified by FTIR measurement. As illustrated in Figure 2b, this plastic waste has a typical spectrum of polypropylene (PP): the IR absorption peaks at 2837 cm^{-1} and 2920 cm^{-1} are attributed to the CH_2 symmetric and asymmetric stretches, respectively [15]; the absorption peak located at 1450 cm^{-1} is characteristic of CH_2 scissor vibrations; the peak at around 1376 cm^{-1} belongs to the CH_3 symmetric deformation vibrations; and other peaks found in the lower frequency region from 1000 to 840 cm^{-1} are attributed to C–C asymmetric and symmetric stretching [16]. These typical spectrum bands of PP revealed that this plastic waste is primarily constituted of elements C and H [17], which could be a good resource of CH_4 for steel carburization under high temperature. The detailed elemental composition of snack packaging plastics waste was determined by LECO, ICP-OES, and ICP-MS. As given in Table 2, the elemental investigation demonstrates that the carbon content in this plastic waste has reached up to 90.2%, followed by N element at 0.40%, and Al element at 4153 mg/kg.

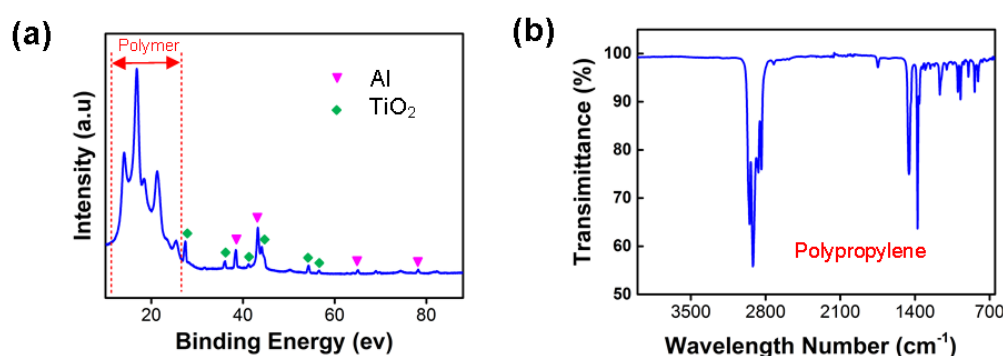


Figure 2. (a) XRD pattern for the snack packaging plastics waste and (b) FTIR spectrum for the snack packaging plastics waste.

Table 2. Elemental composition of snack packaging plastic waste.

Ultimate Analysis		
C	90.4	wt. %
N	0.4	
S	0.04	
Al	4153	mg/kg
Ca	419	
Cu	309	
P	203	

3.2. Mechanism of Steel Carburization by Using Plastic Waste as a Carbon Resource

The thermal degradation behavior of snack chips packaging plastic waste investigated by TGA is shown in Figure 3a. It gives an overall decomposition performance of plastic waste. The mass loss

TGA and differential thermal analysis (DTG) curves demonstrate that snack chips packaging plastic waste has only one degradation step by the presence of one single peak in the DTG curve. The major decomposition started at around 388 °C and ended at approximate 490 °C; the maximum degradation rate was achieved at temperature of 463 °C with a calculated degradation rate of 26.82 wt. %·min⁻¹. When the pyrolyzing temperature was increased to 500 °C, 93% of the waste was vaporized and left 7% of the waste as a final residue. In the following increase of pyrolyzing temperature process, no further weight changes of the residue can be observed implying the completion of plastic gasification at a temperature of 500 °C.

When a steel sample was heated together with some plastic waste under a carburization temperature of 1200 °C, two types of reaction would be involved in this process. One is the pyrolytic gasification of plastic waste and the other is the carburization reaction between steel and the gaseous products decomposed from plastic waste.

The pyrolytic gasification reaction will mainly refer to the degradation of the packaging plastics waste, which can be expressed as:



As the polymer type contained in the plastic waste is polypropylene, which is constituted of methyl groups [18], the released volatiles will primarily be composed of hydrocarbon gases like methane, ethane, propane, and ethylene, etc. [19] and the amount of smaller molecular gases will increase with the rising of the pyrolytic temperature [20]. At a temperature of 1200 °C, the smallest monomer hydrocarbon gas, methane, would dominate the whole gas emission system as more secondary cracking reactions will occur at this temperature to facilitate further hydrocarbon gas decomposition.

Methane is one of the main conventional carbon resources used for steel carburization. During the carburization process, methane will deposit on the steel surface and react with the steel as [2,21]:



Fe(C) represents the carbon solution in austenite (γ -Fe).

Through this gas-solid chemical reaction, carbon from methane will be deposited on the steel surface and be absorbed to increase the carbon content of steel.

In addition to methane, carbon monoxide, which could be decomposed from food contamination, like carbohydrates, is also a good carbon resource for steel carburization. Carbon monoxide will react with steel as:



Considering the hydrogen generated from reaction 1, the reaction between carbon monoxide and steel will be further enhanced by:

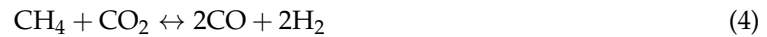


At high temperature, these reactions are all reversible. The reduction gas components, CO, CH₄, and H₂, facilitate carbon solution into iron to form Fe(C), leading to carburization; while oxidizing gases, CO₂, and H₂O, negatively carry the carbon off from Fe(C) to cause decarburization. The overall direction of these reactions depends on their corresponding equilibrium constants and gas composition in the whole atmosphere.

In this study, the continuous liberation of CH₄, CO, and CO₂ gases from the pyrolysis of packaging plastics waste at a temperature of 1200 °C was monitored by an IR gas analyzer. As illustrated in Figure 3b, the emission of reduction gases CH₄ and CO is far beyond the release of oxidizing gas CO₂ in this process. The dominant emission of CH₄ and CO from snack packaging waste will significantly

facilitate the reactions proceeding in the steel carburization direction which, theoretically, evidenced the potential of utilizing snack packaging plastic waste as a carburization agent for steel.

In addition, CH₄ can also react with CO₂ and H₂O, leading to the generation of reducing gases, CO and H₂, to enhance the carburization process proceeding further:



Additionally, the existence of aluminum in the packaging plastic, as discussed in the XRD section, will also contribute to the building of reducing gas atmosphere for steel carburization as [22]:



Above all, the pyrolytic characteristic of snack packaging plastics waste provided the theoretical basis to be used as a carbon precursor for steel carburization.

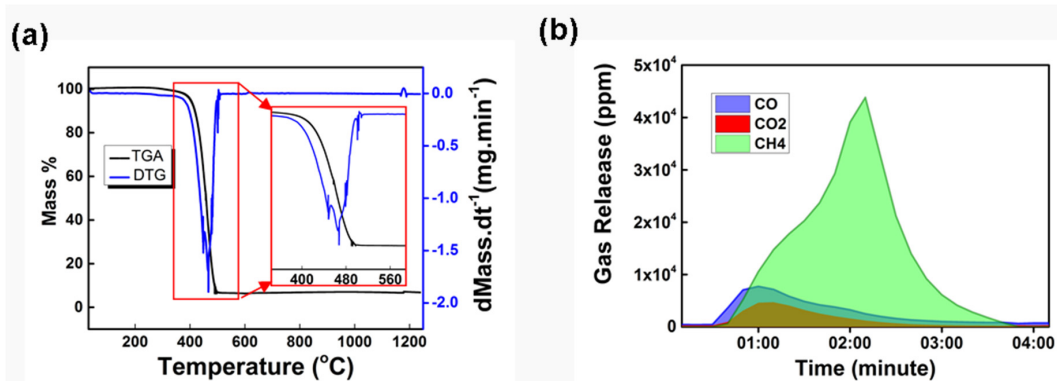


Figure 3. (a) TGA-DTG curve for the snack packaging plastics waste. (b) IR gas analysis for the gases emission from plastic waste at 1200 °C.

3.3. Characterisation for the Carburization Effect of Metallized Plastics Waste on Steel

The steel microstructure depends highly on its carbon content [2]. The microstructure of carburized steel usually gives a different structure constitution with the raw material as more carbon is absorbed for a higher carbon content. Figure 4 illustrates a microstructure comparison between the reference steel sample and the as-carburized steel sample. Figure 4a1 is the overview microstructure (50×) for the reference steel sample with a carbon content of 0.39 wt. %. It has a homogenous ferrite-pearlite steel constituent [23,24] which gives a microstructure of some pearlite with a few pro-eutectoid ferrite phases lying along the prior austenite grain boundary. In this microstructure, ferrite is a carbon-poor phase which is in a body-centered cubic form of iron with a maximum carbon solubility of 0.02 wt. % at 723 °C and 0.001% at 0 °C [25]; pearlite is a lamellar two-phase microstructural constituent with alternating layers of ferrite and cementite [26,27], which is a carbon-rich phase with an orthorhombic unit containing 12 iron atoms and four carbon atoms having a formula of Fe₃C as well as 6.67% carbon by weight [28]. With the increase of carbon content in steel sample, the volume fraction of ferrite will decrease but the volume fraction of cementite will increase which in turn further increases the volume fraction of pearlite [29]. Figure 4b1 gives the overview microstructure (50×) of the as-carburized steel sample treated with plastic waste at a temperature of 1200 °C over 10 min. It can be clearly seen that the volume fraction of carbon-poor ferrite phase got significantly reduced but carbon rich pearlite structure got dramatically increased, which indicated an increase of carbon content in steel. Furthermore, the microstructure located at the outer surface of the as-carburized steel sample demonstrated a typical eutectoid pearlite microstructure equivalent to a steel sample with carbon

content around 0.7 wt. % [2,26]. Figure 4(a2, b2) gives a detailed microstructure comparison (500 \times) between the reference steel sample and the as-carburized steel sample. It can be observed that the volume fraction of carbon-poor proeutectoid ferrite phase on the reference steel sample is much more than that in the as-carburized steel sample, which was also verified by the higher magnification (3000 \times) investigation of SEM as shown in Figure 4(a3,b3). The significant increase of volume fraction for pearlite structure and decrease of ferrite phase on the surface of as-carburized steel sample implies the increase of carbon content on the steel surface. This evidenced the carbon rich reducing gas liberated from snacking packaging as discussed in the mechanism section did react with the steel sample and led to a significant carburization effect on the steel surface.

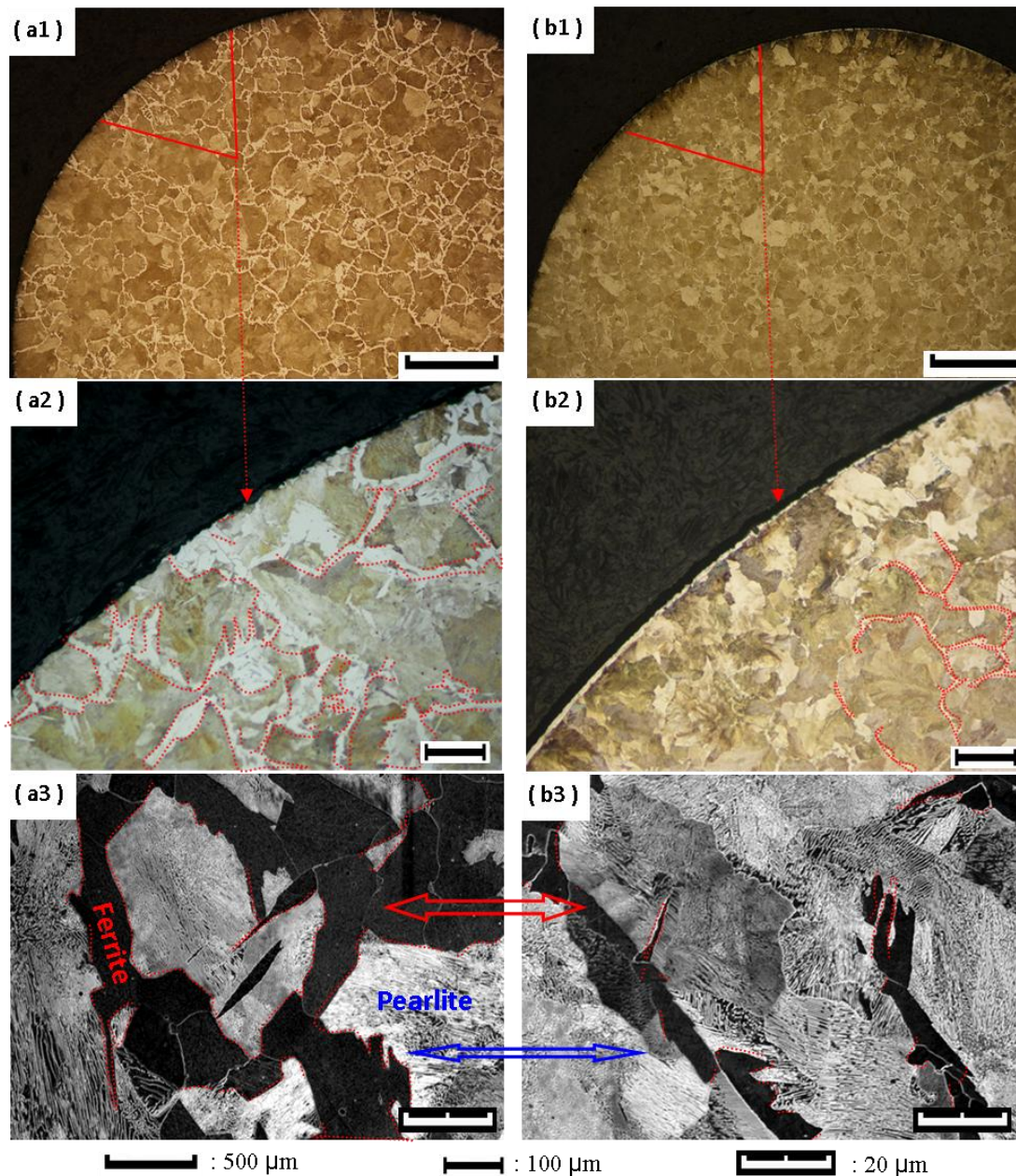


Figure 4. (a1–a3) Microstructure for the reference steel sample under magnifications of 50 \times , 500 \times , and 3000 \times . (b1–b3) Microstructure for the as-carburized steel sample under magnifications of 50 \times , 500 \times , and 3000 \times .

To further understand the high-temperature reactions occurring between the plastic waste and the steel sample, the chemical state of carbon, aluminum, titanium, as well as the carbon content against the depth profile of the as-carburized steel surface were determined by the XPS technique. The sample was firstly ultrasonically cleaned in acetone for 5 min to eliminate hydrocarbon contamination at the surface. Then the selected area of analysis was ion beam sputtered for 12 min at a rate of 0.3 nm per second for carbon distribution analysis. A total of six layers of surface carbon analysis was conducted after various etching times, including 0 s (top surface), 60 s, 180 s, 300 s, 420 s, and 720 s etching, corresponding to the depth of 0 nm (top surface) 18 nm, 54 nm, 90 nm, 126 nm, and 216 nm, respectively. The detailed C 1s spectrum deconvolution, as given in Figure 5a, shows that C 1s were mainly composed of two fitted components: the predominant C 1s_A peaked at 283.0 eV corresponding to the compound of carbide and a small peak C 1s_B fitted at 284.1 eV relevant to the other form of carbon [30,31]. The specific carbon content against the depth (etching time) profile, as illustrated in Figure 5b, revealed an obvious carbon gradient with distinctly higher surface carbon concentration detected on as-carburized steel. Considering the carbon mainly exists as a compound of carbide (peak C 1s_A), this increased carbon content would have the capability to create a corresponding microstructure evolution as observed in the microscopy investigation section.

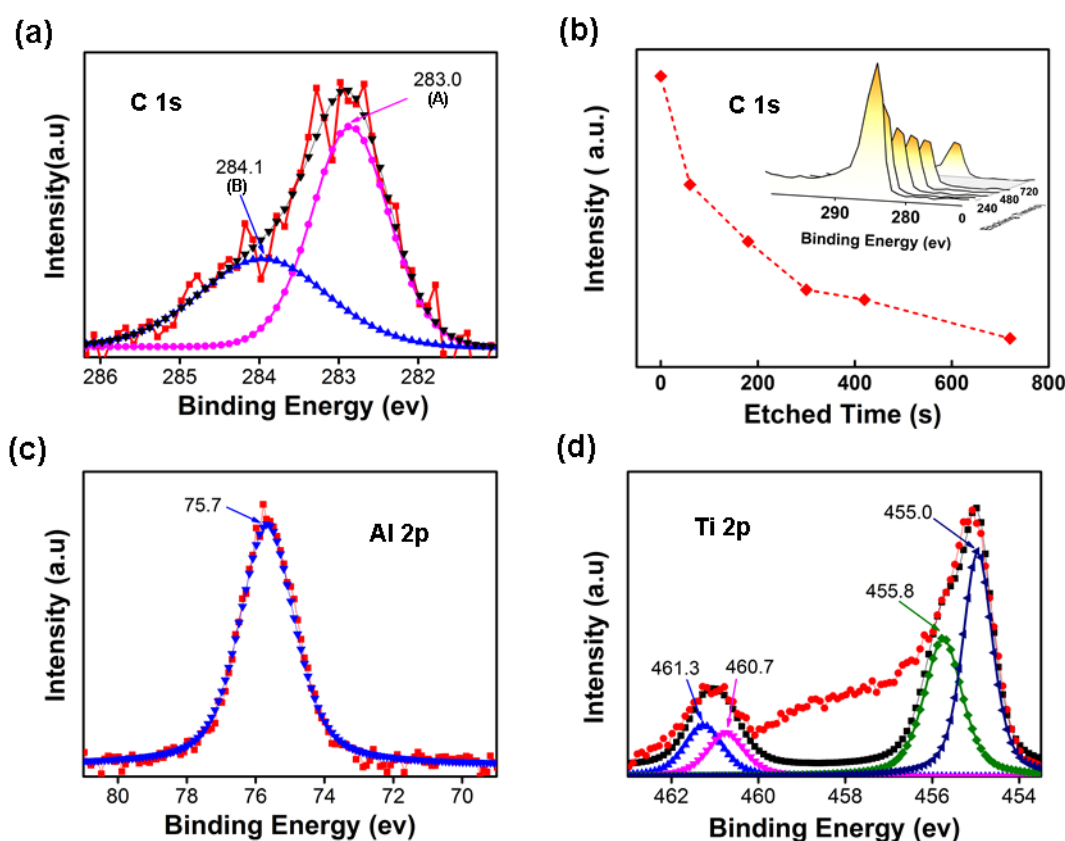


Figure 5. (a) C 1s spectrum for the carbon contained in the as-carburized steel; (b) relative carbon intensity against the depth (etched time) profile in the as-carburized steel. (c) Al 2p spectrum for the carbon contained in the as-carburized steel; and (d) the Ti 2p spectrum for the carbon contained in the as-carburized steel.

In view of the existence of aluminum and titanium dioxide in the plastic waste, as mentioned in the XRD investigation, high-temperature reactions relevant to aluminum and titanium might also be involved in this process and left some reaction products on the steel surface. Thus, the chemical state of aluminum and titanium on the as-carburized steel surface were also analyzed by XPS. As shown in Figure 5c, the aluminum detected on the steel surface is found in the Al–O state peaked at 75.7 eV,

referring to aluminum oxide [32], which showed that the reaction between aluminum and carbon dioxide did occur as discussed in the mechanism section. This reaction can not only help to build a reducing gas atmosphere for steel carburization, but can also enhance the steel wear and corrosion resistance with the introduction of surface alumina [33]. The Ti 2p spectrum detected on the steel surface is given in Figure 5d. It can be deconvoluted into four peaks at 461.3 eV, 460.7 eV, 455.5 eV, and 455.0 eV, which correspond to Ti_2O_3 , TiN_x , TiN, and TiN_xO_y , respectively [34]. These different forms of titanium oxides and nitrides revealed the carbothermal reduction of titanium dioxide, as well as its nitridation attributed to the presence of carbon and nitrogen in plastic waste as determined in the ICP analysis [35]. Similarly, these titanium nitrides deposited on the steel surface could also provide good protection for steel against wear and corrosion.

To accurately estimate the carburization effect of snack packaging plastic waste on steel, the EPMA technique was adapted to quantitatively investigate the accurate carbon content against the depth distribution on the as-carburized steel. As shown in Figure 6, the carbon content from the steel surface to the center of the as-carburized steel sample and the reference steel sample (raw material) were both analyzed by EPMA. It is obvious that the carbon distribution on the reference steel sample gives a minor fluctuation from steel surface to the center, averaging 0.39 wt. % with a standard derivation of 0.02 wt. %. This result is consistent with its bulk calibration carbon content (0.39 wt. %) and homogenous ferrite-pearlite microstructure as observed from OM and SEM studies. Different with the uniform fluctuation on the reference material, the carbon distribution on the as-carburized steel sample demonstrated a significant carbon gradient as given in Figure 6. The highest carbon content on the steel surface reached 0.72 wt. %, which approximates the carbon content of eutectoid steel [36] as discussed in the microscopy investigation section. Additionally, it can also be clearly seen that the carbon concentration higher than 0.55 wt. % has extended to a depth of 0.3 mm, giving a significant case surface with relatively higher carbon concentration in agreement with the microstructure observation mentioned above.

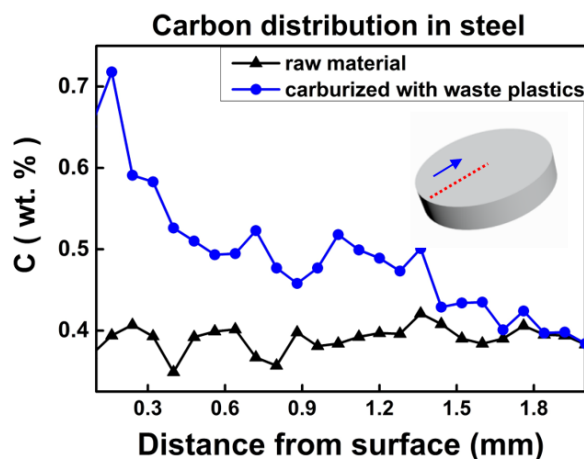


Figure 6. Detailed carbon concentration distribution in the reference steel sample and the as-carburized steel sample.

4. Conclusions

In this research, a sustainable approach to utilize post-consumer snack packaging plastic as a carbon resource for steel carburization is investigated. When treating a steel sample together with some packaging plastic waste in a horizontal tube furnace under a temperature of 1200 °C, a considerable amount of carbon-rich reducing gases, CO and CH_4 , were released from the snack packaging plastic waste and served as carburization agents for steel carburizing. The carburization effect of plastic waste on the steel was investigated by the techniques of OM, SEM, XPS, and EPMA. All the investigation results revealed the snack chips packaging plastic waste did effectively work as a carbon precursor

for steel carburization by giving rise to a remarkable increase of surface carbon concentration and the corresponding microstructure evolution formed on the steel surface. Additionally, the aluminum and titanium dioxide contained in the plastic waste also took part in the high-temperature reactions in this system and left alumina and titanium nitride ceramics on the steel surface to provide further protection for steel against wear and corrosion. This sustainable steel carburization approach could not only alleviate the consumption of natural gas used in the conventional gas carburization of steel, but can also significantly reduce the accumulation of plastics waste.

Acknowledgments: This research was supported under Australian Research Council's Industrial Transformation Research Hub Funding Scheme (Project No. IH130200025).

Author Contributions: Songyan Yin performed the experiments, analyzed the data, and wrote the whole manuscript; Ravindra Rajarao and Farshid Pahlevani designed the experiments; and Veena Sahajwalla provided paper revision and funding.

Conflicts of Interest: The authors declare no conflict of interest.

References

1. Tobie, T.; Hippenstiel, F.; Mohrbacher, H. Optimizing Gear Performance by Alloy Modification of Carburizing Steels. *Metals* **2017**, *7*, 415. [[CrossRef](#)]
2. Gray, A. *Carburizing and Carbonitriding*; ASM: Metals Park, OH, USA, 1977.
3. Sugimoto, K.-I.; Hojo, T.; Mizuno, Y. Effects of vacuum-carburizing conditions on surface-hardened layer properties of transformation-induced plasticity-aided martensitic steel. *Metals* **2017**, *7*, 301. [[CrossRef](#)]
4. Thompson, M.; Davison, M.; Rasmussen, H. Natural gas storage valuation and optimization: A real options application. *Nav. Res. Logist.* **2009**, *56*, 226–238. [[CrossRef](#)]
5. Das, P.; Tiwari, P. Valorization of packaging plastic waste by slow pyrolysis. *Resour. Conserv. Recycl.* **2018**, *128*, 69–77. [[CrossRef](#)]
6. Yao, D.; Zhang, Y.; Williams, P.T.; Yang, H.; Chen, H. Co-production of hydrogen and carbon nanotubes from real-world waste plastics: Influence of catalyst composition and operational parameters. *Appl. Catal. B Environ.* **2018**, *221*, 584–597. [[CrossRef](#)]
7. Bosmans, A.; Vanderreydt, I.; Geysen, D.; Helsen, L. The crucial role of Waste-to-Energy technologies in enhanced landfill mining: A technology review. *J. Clean. Prod.* **2013**, *55*, 10–23. [[CrossRef](#)]
8. Iranpour, R.; Stenstrom, M.; Tchobanoglous, G.; Miller, D.; Wright, J.; Vossoughi, M. Environmental engineering: Energy value of replacing waste disposal with resource recovery. *Science* **1999**, *285*, 706–711. [[CrossRef](#)] [[PubMed](#)]
9. Zaman, A.U. A comprehensive study of the environmental and economic benefits of resource recovery from global waste management systems. *J. Clean. Prod.* **2016**, *124*, 41–50. [[CrossRef](#)]
10. Marsh, K.; Bugusu, B. Food packaging—Roles, materials, and environmental issues. *J. Food Sci.* **2007**, *72*, R39–R55. [[CrossRef](#)] [[PubMed](#)]
11. Barlow, C.; Morgan, D. Polymer film packaging for food: An environmental assessment. *Resour. Conserv. Recycl.* **2013**, *78*, 74–80. [[CrossRef](#)]
12. Achilias, D.; Giannoulis, A.; Papageorgiou, G. Recycling of polymers from plastic packaging materials using the dissolution—Reprecipitation technique. *Polym. Bull.* **2009**, *63*, 449–465. [[CrossRef](#)]
13. Mo, Y.; Zhao, L.; Wang, Z.; Chen, C.L.; Tan, G.Y.A.; Wang, J.Y. Enhanced styrene recovery from waste polystyrene pyrolysis using response surface methodology coupled with Box-Behnken design. *Waste Manag.* **2014**, *34*, 763–769. [[CrossRef](#)] [[PubMed](#)]
14. Chen, X.; Mao, S.S. Titanium dioxide nanomaterials: Synthesis, properties, modifications, and applications. *Chem. Rev.* **2007**, *107*, 2891–2959. [[CrossRef](#)] [[PubMed](#)]
15. Zhang, D.; Shen, Y.; Somorjai, G.A. Studies of surface structures and compositions of polyethylene and polypropylene by IR+ visible sum frequency vibrational spectroscopy. *Chem. Phys. Lett.* **1997**, *281*, 394–400. [[CrossRef](#)]
16. Morent, R.; De Geyter, N.; Leys, C.; Gengembre, L.; Payen, E. Comparison between XPS- and FTIR-analysis of plasma-treated polypropylene film surfaces. *Surf. Interface Anal.* **2008**, *40*, 597–600. [[CrossRef](#)]
17. Busico, V.; Cipullo, R. Microstructure of polypropylene. *Prog. Polym. Sci.* **2001**, *26*, 443–533. [[CrossRef](#)]

18. Arkatkar, A.; Arutchevi, J.; Bhaduri, S.; Uppara, P.V.; Doble, M. Degradation of unpretreated and thermally pretreated polypropylene by soil consortia. *Int. Biodeterior. Biodegrad.* **2009**, *63*, 106–111. [[CrossRef](#)]
19. Hedrick, S.A.; Chuang, S.S. Temperature programmed decomposition of polypropylene: In situ FTIR coupled with mass spectroscopy study. *Thermochim. Acta* **1998**, *315*, 159–168. [[CrossRef](#)]
20. Park, J.J.; Song, H.-J.; Park, J.-W. The behaviors of H₂, CH₄, C₂H₄ and C₃H₆ from the decomposition of polypropylene by NiO/Si-Al catalyst. *J. Mater. Cycles Waste Manag.* **2013**, *15*, 37–41. [[CrossRef](#)]
21. Kwietniewski, C.E.; Tentardini, E.K.; Totten, G.E. Carburizing and Carbonitriding. In *Encyclopedia of Tribology*; Springer: Berlin, Germany, 2013; pp. 298–306.
22. Gjerstad, S.; Welch, B. Oxidation of Aluminum by Carbon Dioxide in the Presence of Cryolitic electrolyte. *J. Electrochem. Soc.* **1964**, *111*, 976–980. [[CrossRef](#)]
23. Zhang, S.; Zhao, H.; Shu, F.; He, W.; Wang, G. Microstructure and Corrosion Behavior of Simulated Welding HAZ of Q315NS Steel in Sulfuric Acid Solution. *Metals* **2017**, *7*, 194. [[CrossRef](#)]
24. Parsons, S.; Edmonds, D. Microstructure and mechanical properties of medium-carbon ferrite-pearlite steel microalloyed with vanadium. *Mater. Sci. Technol.* **1987**, *3*, 894–904. [[CrossRef](#)]
25. Smith, W.F.; Hashemi, J. *Foundations of Materials Science and Engineering*; McGraw-Hill: New York, NY, USA, 2011.
26. Gladshstein, L.; Larionova, N.; Belyaev, B. Effect of ferrite-pearlite microstructure on structural steel properties. *Metallurgist* **2012**, *56*, 579–590. [[CrossRef](#)]
27. Toribio, J.; González, B.; Matos, J.C.; Ayaso, F.J. Influence of Microstructure on Strength and Ductility in Fully Pearlitic Steels. *Metals* **2016**, *6*, 318. [[CrossRef](#)]
28. Zhou, D.; Shiflet, G. Ferrite: Cementite crystallography in pearlite. *Metall. Mater. Trans. A* **1992**, *23*, 1259–1269. [[CrossRef](#)]
29. Samuels, L.E. *Optical Microscopy of Carbon Steels*; American Society for Metals: Metals Park, OH, USA, 1980.
30. Chastain, J.; King, R.C.; Moulder, J. *Handbook of X-Ray Photoelectron Spectroscopy: A Reference Book of Standard Spectra for Identification and Interpretation of XPS Data*; Physical Electronics Division, Perkin-Elmer Corporation: Eden Prairie, MN, USA, 1992.
31. Lopez, D.; Schreiner, W.H.; De Sánchez, S.R.; Simison, S.N. The influence of carbon steel microstructure on corrosion layers: An XPS and SEM characterization. *Appl. Surf. Sci.* **2003**, *207*, 69–85. [[CrossRef](#)]
32. Whangbo, S.; Choi, Y.K.; Jang, H.K.; Chung, Y.D.; Lyo, I.W.; Whang, C.N. Effect of oxidized Al prelayer for the growth of polycrystalline Al₂O₃ films on Si using ionized beam deposition. *Thin Solid Films* **2001**, *388*, 290–294. [[CrossRef](#)]
33. Jeurgens, L.; Sloof, W.G.; Tichelaar, F.D.; Mittemeijer, E.J. Structure and morphology of aluminium-oxide films formed by thermal oxidation of aluminium. *Thin solid films* **2002**, *418*, 89–101. [[CrossRef](#)]
34. Braic, M.; Braic, V.; Balaceanu, M.; Kiss, A.; Cotrut, C.; Drobe, P.; Vladescu, A.; Vasilescu, C. On Some Characteristics of Ti Oxynitrides Obtained by Pulsed Magnetron Sputtering. *Plasma Process. Polym.* **2007**, *4*, S171–S174. [[CrossRef](#)]
35. Yin, S.; Rajarao, R.; Kong, C.; Wang, Y.; Gong, B.; Sahajwalla, V. Sustainable Fabrication of Protective Nanoscale TiN Thin Film on a Metal Substrate by Using Automotive Waste Plastics. *Sustain. Chem. Eng.* **2016**, *5*, 1549–1556. [[CrossRef](#)]
36. Bhadeshia, H.; Honeycombe, R. *Steels: Microstructure and Properties*; Butterworth-Heinemann: Oxford, UK, 2017.

